Climate Dynamics (2003) 20: 229–239
DOI 10.1007/s00382-002-0276-2

B. Bhaskaran · A.B. Mullan

El Niño-related variations in the southern Pacific atmospheric circulation: model versus observations

Received: 1 December 2000 / Accepted: 2 July 2002 / Published online: 2 October 2002

Abstract Our objective is two-fold: (1) to study the influence of tropical Pacific sea surface temperature (SST) anomalies associated with the El Niño – Southern Oscillation (ENSO) on the southern Pacific atmospheric circulation using observations; and (2) to assess the ability of a fully comprehensive GCM to reproduce the observed ENSO-related variations. The observed circulation features were derived from the National Center for Environmental Prediction (NCEP) reanalyses of observations. The GCM used is the atmospheric component of the United Kingdom Meteorological Office (UKMO) unified model (UM). A detailed study of the impact of the ENSO on the seasonal mean circulation and on the intraseasonal variability on synoptic time scales has been carried out using both the model and NCEP data for austral summer season. We have also investigated the relationship between the high frequency (HF) transients and the quasi-stationary mean circulation during selected ENSO years. A regional Hadley cell intensity in the tropical Pacific has been used as an El Niño index to classify the warming and cooling years for our composite analysis. During El Niño years the regional Hadley cell acts as a medium through which the enhanced equatorial convection forces a train of Rossby waves to produce the quasi-stationary circulation anomalies in extratropics. The Hadley cell weakens during La Niña years, and the equatorial convection moves further westwards. The Rossby wave response to this situation is to reverse the phase of the quasi-stationary circulation anomalies by 180°, as expected. These features are fairly well simulated by the UM, though the extratropical circulation anomalies in response to the equatorial convection is found about 30° longitude further eastwards than observed during El Niño years. The model confirms the observational evidence that the storm track variations in the southern subtropical Pacific are largely driven by variations in the South Pacific Convergence Zone (SPCZ) associated with the El Niño and La Niña events. However the model struggles to reproduce the significant storm track activity, present in the NCEP data, related to the westerly jet stream during La Niña years. Finally, the relationship between the HF transients and the quasi-stationary anomalies found in both the model and observations supports the role of the HF transients in forcing the time-mean circulation, as reported by Hoerling and Ting 1994 for the Pacific – North American (PNA) region.

B. Bhaskaran (✉) · A.B. Mullan
National Institute of Water and Atmospheric Research,
PO Box 14901, Greta Point, Wellington, New Zealand
E-mail: b.bhaskaran@niwa.cri.nz
Fax: +64-4-386 2153

1 Introduction

The impact of sea surface temperature (SST) variations in the tropical Pacific associated with the El Niño – Southern Oscillation (ENSO) cycle has been a subject of intense investigations over the last decade (Philander 1990). An important reason for this strong interest has been due to the changes in the circulation features observed worldwide during El Niño years (Walker and Bliss 1937; Bjerknes 1969; Ropelewski and Halpert 1989). In recent years the ENSO research has been carried out with a view to improve seasonal forecasting, since the ENSO-induced changes in the large-scale circulations are potentially predictable (Latif et al. 1998). Therefore it is important not only to understand the ENSO-related circulation features, but also to assess a fully comprehensive general circulation model's (GCM's) ability to reproduce these observed ENSO-related features.

The focus is on the response of the southern subtropics and extratropics to variations in tropical Pacific SSTs. The current view of how these teleconnections often operate is that tropical SSTs influence the extratropics indirectly through the medium of regional

Hadley circulations. Anomalous SSTs generate changes in tropical convection which alter upper level divergence and the meridional overturning of regional Hadley cells (Rasmusson and Mo 1993; Trenberth et al. 1998). The upper level convergence in the subtropics near the descending branch of the Hadley circulation acts as a source of Rossby waves (Sardeshmukh and Hoskins 1988) that then propagate downstream in the midlatitude westerlies. Rasmusson and Mo (1993) discuss this concept of a *regional* Hadley cell, which departs from the classical picture of the Hadley circulation being a zonally averaged feature of the global climate. They argued that a regional Hadley cell was a useful concept, and could be applied quantitatively provided the meridional overturning was calculated using only the *divergent* component of the wind. This follows from the formalism of Sardeshmukh and Hoskins (1988) who partitioned the wind field in the vorticity equation into rotational and divergent components: the rotational wind component was essential to the existence and propagation of Rossby waves, whereas only the divergent component entered into the right-hand source term defined as the Rossby wave source.

An additional factor in understanding the amplitude and pattern of (steady) extratropical responses to tropical heating is the interaction of high frequency (HF) transient eddies with the mean flow. Extratropical anomalies from ENSO SST variations have been observed to have preferred geographic locations, and it has been suggested (Hoerling and Ting 1994) that this is due partly to the effect of the transient eddies (e.g. a consequence of the elongated jet stream in the Northern Hemisphere during El Niño periods).

The ENSO-induced variations in the *Northern* Hemisphere regional circulations have been extensively investigated using both models and observations (Trenberth et al. 1998; Kane 1998; Hoerling et al. 1997). However, similar comprehensive analyses for the Southern Hemisphere regional domains have been limited. For example, studies on the ENSO-related changes in the circulation features over the Australia–New Zealand (ANZ) region were largely confined to the observational analyses alone (McBride and Nicholls 1983; Gordon 1986; Mullan 1996). Even in these studies, the authors mainly discussed the ENSO impact only on the mean circulation using monthly or seasonal mean values (stationary response). A very few papers have addressed the transient response on synoptic time scales to ENSO (but see e.g. Renwick 1998).

We therefore undertake a comprehensive study of the impact of the ENSO on the seasonal mean flow and on the intraseasonal variability on synoptic time scales in the southern Pacific using the National Center for Environmental Prediction (NCEP) reanalyses of observations. We will also investigate the interaction of the synoptic scale transient eddies with the seasonal mean circulation during El Niño and La Niña events. Subsequently the ability of a fully comprehensive GCM developed at the United Kingdom Meteorological Office (UKMO) to reproduce the observed circulation features associated with the ENSO will be assessed. The organization is as follows: in Sect. 2 we describe the data and methodology used in our study. The Hadley cell intensity index used to select the El Niño and La Niña events is also described in Sect. 2. Sections 3 and 4 describe the observed and modelled El Niño-related variability. Summary and conclusions follow in Sect. 5.

2 Data and methods

2 Data description and filtering

2.1.1 Observations

The observed circulation features for the El Niño and La Niña cases during the period 1960–94 were derived from the NCEP reanalyses of observations. To compute the regional Hadley cell, we have used monthly means of meridional divergent winds at 10 pressure levels: 1000, 925, 850, 700, 600, 500, 400, 300, 200, and 100 hPa. In order to study the interannual variations associated with the tropical Pacific SST anomalies, a band pass filter has been used to retain variability on ENSO time scale. For single level analyses we preferred to use the 300 hPa level because it remains in the upper troposphere at all latitudes and hence more directly relates to vorticity sources in the divergent flow. The transient eddy kinetic energy in the time scale of 2.5–8 days, a measure of the synoptic scale storm activity, has been calculated using a band pass filtered u and v wind components at 300 hPa. The computation of transient vorticity forcing anomalies also utilizes the 300 hPa band pass filtered wind components. The band pass filter used here is a second-order Butterworth filter suggested by Murakami (1979). The advantage of using this filter is that there is no serious cutoff problem at the ends of the time series, since only two points outside the range of the input data are needed to calculate the output. This property was particularly useful when we used a short (90-day) time series of daily data to calculate seasonal transient eddy kinetic energy and transient vorticity forcing anomalies for austral summer.

A monthly global precipitation dataset for land areas prepared at the Climate Research Unit (CRU) has been used to build the ENSO composites to validate the model precipitation. The techniques used to construct the gridded dataset at 2.5° × 3.75° resolution using station observations and other related details can be found in Hulme (1992).

Finally, the Nino3.4 sea surface temperature anomaly time series is used as an indicator of the ENSO variability in the tropical Pacific. The Nino3.4 region is bounded by the latitudes 5°S–5°N and longitudes 170°–120°W. The anomalies are calculated with respect to the annual cycle using a 2.3b version of the GISST dataset (Parker et al. 1995).

2.1.2 The unified model

The model used here is the atmospheric component of the unified model (UM) developed at the United Kingdom Meteorological Office, UK (Cullen 1993). The global atmosphere is represented by a hydrostatic primitive equation grid point model containing 19 vertical levels. Regular latitude–longitude grid resolution of 2.5° × 3.75° is employed. The governing equations are solved using split-explicit finite difference scheme at 30 min intervals. For more extensive details of the model the reader is referred to Stratton (1999) and Bhaskaran et al. (1996). The model has been integrated for 35 years starting from 1 August 1960. The 2.3b version of the GISST dataset (Parker et al. 1995) has been used to force the model at the sea surface (see Bhaskaran et al. 1999 for more details). All the data

corresponding to the NCEP reanalyses fields described in Subsect. 2.1.1 were generated by the UM. The daily data have been created using twice-daily model simulated fields, whereas 6-h data have been used to form daily means for the NCEP reanalyses.

2.2 Hadley circulation

A measure of the strength of the regional Hadley cell (ψ) in the western tropical Pacific region [150°E–150°W; and 10–20°S] has been calculated using the relation

$$\psi = [\overline{v_{200}}] - [\overline{v_{850}}] \ ,$$

where v_p is meridional divergent wind at pressure level p. The operators ($\bar{}$) and [ ] refer to temporal and spatial averaging.

2.3 Rossby wave source

Total Rossby wave source has been calculated following Sardeshmukh and Hoskins (1988) and Rasmusson and Mo (1993) using the relation

$$\bar{S} = -\overline{(\xi + f)\nabla \cdot V_\chi} - \overline{V_\chi \cdot \nabla(\xi + f)} \ .$$

The symbol ($\bar{}$) refers to time mean, ξ is the relative vorticity, f is the coriolis parameter, and V_χ is the divergent wind vector. The first term on the right-hand-side is the vortex-stretching term, and the second term represents the advection of absolute vorticity by the divergent wind.

2.4 Transient eddy kinetic energy

The transient eddy kinetic energy (teke) has been calculated using the relation $teke = (u_f^2 + v_f^2)/2$. Here u_f and v_f are the band pass filtered wind components in the time scale of 2.5–8 days. This transient eddy kinetic energy is used as an indicator of the synoptic scale wave activity.

2.5 Vorticity flux convergence tendency

Streamfunction tendency due to the high frequency transient vorticity flux convergence (Hoerling and Ting 1994) is defined as

$$T = -\nabla^{-2}\left[\frac{\partial}{\partial x}\left(\overline{u_f \xi_f}\right) + \frac{\partial}{\partial y}\left(\overline{v_f \xi_f}\right)\right] \ ,$$

where u_f and v_f are the filtered high frequency wind components, and ξ_f represents the filtered high frequency vertical component of the relative vorticity. Thus the positive (negative) values of T indicate a cyclonic (anticyclonic) forcing due to high frequency (HF) transients in the Southern Hemisphere.

2.6 Compositing procedure

A number of earlier studies to document the El Niño – related variability in the circulation features over the ANZ region (e.g. Mullan 1996; Power et al. 1998) have used the Southern Oscillation Index (SOI) to classify the El Niño and La Niña events. The SOI may be considered as a measure of the direct tropical atmospheric response to the equatorial Pacific SST anomalies associated with the El Niño and La Niña events. However, the impact of El Niño on the extratropical circulation is indirect, and may be viewed in terms of the regional Hadley circulation anomalies (Rasmusson and Mo 1993). Moreover, the series of SOI obtained from a GCM based NCEP reanalyses data may not reflect the true observed SOI, since the current GCMs are not accurate enough to reproduce the observed grid-point statistics. In the following subsection therefore we justify the use of the western Pacific regional Hadley cell intensity as an El Niño index to identify the warming and cooling events.

2.6.1 Hadley – El Niño time series

The monthly time series of ψ for the western tropical Pacific has a stronger multiannual component, relative to those for other domains in the tropical Pacific, over which the seasonal cycles are superimposed (not shown). This suggests that the regional Hadley cell in this region has a stronger relationship with El Niño events. In order to establish this relationship, we have plotted the western Pacific Hadley cell intensity time series (ψ-values) along with the time series of nino3.4 SST anomalies in Fig. 1. Both the series were filtered to retain variability in the time scale of 26–47 months. Note that with the standard sign convention (see Sect. 2.2), a stronger meridional regional Hadley cell has enhanced southward flow at 200 hPa (more negative v_{200}), and hence ψ is more negative. It can be seen that the increased intensities of the Hadley cell are largely associated with the warm phases of the ENSO cycles, while the weakened Hadley cell intensities are related to the cold phases, as theorized many years ago by Bjerknes (1966, 1969). Therefore it is appropriate to use the western Pacific regional Hadley cell intensity index (ψ) as a measure of atmospheric response to ENSO. Hereafter the terms *Hadley cell* and *regional Hadley cell* will refer to the western Pacific regional Hadley cell.

2.6.2 Event selection

The warm (cold) composite was obtained by averaging DJF seasons where ψ anomalies exceeded 0.75σ (standard deviation) in the negative (positive) direction. This criterion includes most of the nino3.4 SST index based El Niño (La Niña) years in the warm (cold) composite (Table 1). Note also that event selection used the raw streamfunction anomalies, not the low-pass filtered values of Fig. 1. Although fluctuations in the Hadley cell are largely driven by the nino3.4 SST anomalies (see Fig. 1), there were cases during which the Hadley cell was not entirely driven by the SSTs alone. For example, during the austral summer of 1963–64 (1967–68) the nino3.4 SST anomaly was above 0.75σ (below -0.75σ) though the

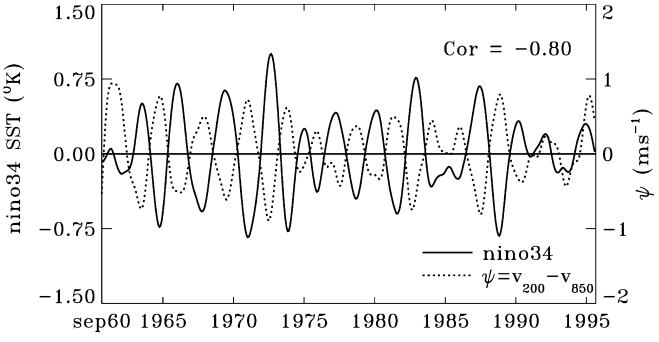

Fig. 1 Time series of sea surface temperature anomalies in the nino3.4 region (5°S–5°N and 170°–120°W) in K, and of tropical Hadley cell intensity $\psi = [\overline{v_{200}}] - [\overline{v_{850}}]$ in the sector (150°E–150°W) in ms^{-1} (see text for details). Both series were band pass filtered in the time scale of 26–47 mon

Table 1 Selected El Niño and La Niña years for our composite analysis

El Niño years	La Niña years
1965–66	1970–71
1968–69	1973–74
1972–73	1975–76
1982–83	1984–85
1986–87	1988–89
1991–92	

Hadley cell intensity was not below -0.75σ (above 0.75σ). This suggests that in some years the tropical Pacific SST signal may not get through to the extratropical atmospheric circulation through the regional Hadley cell. Therefore it makes sense to use the regional Hadley cell intensity index (ψ) to select events for warm and cold composites. Table 1 identifies the warm and cold years based on the ψ-index. Using the nino3.4 SST index would produce the same set, except for the addition of 1963–64 (warm) and 1967–68 (cold).

3 Observed El Niño-related variability

3.1 Interannual variations

In this section we investigate the El Niño-related interannual variations over the ANZ region for austral summer (December–February) season. Figure 2 shows the spatial distribution of contemporaneous correlations between ψ and pressure at mean sea level (PMSL). Note that the correlation is done with the negative of ψ so the polarity is consistent with the warm minus cold composite plots. For a sample of 35 DJF seasons (1960/61–1994/95) the correlation coefficients above 0.28 are significant at 90% level. The structures of the positive and negative correlations confirm the existence of the quasi-stationary Rossby wavetrains forced by the tropical convection (see also Fig. 3). These large-scale quasi-stationary anomalies tend to intensify (weaken) southwesterlies over New Zealand (NZ) during the austral summer of El Niño (La Niña). At mid-latitudes these anomalies assume an equivalent barotropic vertical structure with the same polarity throughout the troposphere, as seen by comparing the correlations of ψ with the mean sea level pressure (Fig. 2) and with 300 hPa height (Fig. 3) anomalies. During El Niño years, the negative 300 hPa height anomalies to the east of NZ resulting from the Rossby wave response appear to induce changes in the jet stream (see Subsect. 3.2.1).

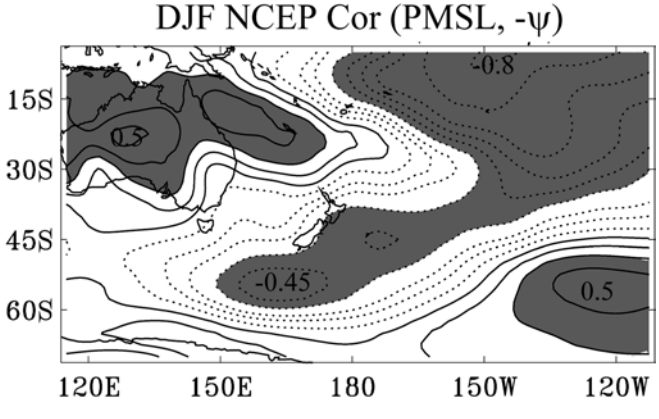

Fig. 2 Spatial distribution of contemporaneous correlation coefficients between regional Hadley cell intensity and pressure at mean sea level obtained from the NCEP data. The contours are drawn at 0.1 intervals, and the non-positive contours are *dotted*. The Correlation coefficients above +0.3 and below –0.3 are *shaded*. Here a sample size of 35 DJF seasons used for which the significant correlation is ±0.28 at 90% level

3.2 Composite analysis results

The observed stationary ENSO response has been investigated using the warm and cold composites of the 300 hPa zonal winds and regional Hadley circulation.

3.2.1 300 hPa zonal wind

The warm and cold DJF composites of 300 hPa winds shown in Fig. 4 are generally in agreement with the quasi-stationary anomalies discussed in Subsect. 3.1. For example, during El Niño years the split in the jet stream over the northeast of NZ (Fig. 4a) appears to be related to the existence of quasi-stationary wave anomalies resulting from the Rossby wave response in this region (see Fig. 3). In general the upper level jet stream has been displaced equatorwards during warm years, especially to the east of the dateline. The higher latitude arm of the jet stream is also substantially weaker east of the dateline in warm years. This has been found to be associated with increased blocking in the far southeast Pacific by Renwick and Revell (1999).

The cold composite largely reinforces the mean climatological DJF pattern with a slight southward shift over the New Zealand longitudes. Changes in the location of the westerly jet stream may have a significant implication for the ANZ region, since the jet stream acts as a storm guide in the Southern Hemisphere extratropics (Trenberth 1991).

3.2.2 Regional Hadley circulation

Although a part of the anomalous upper level outflow associated with the tropical convection is in the form of a Walker circulation, a significant portion is directed polewards. In our analysis, a stronger than normal poleward mass transfer takes place in the form of a regional Hadley cell from the equatorial region (150°E–150°W) during El Niño years. A plot of the

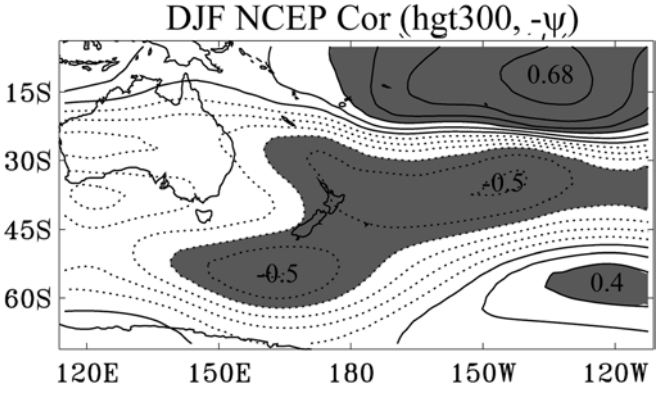

Fig. 3 Same as Fig. 2, but the correlation coefficients were calculated between regional Hadley cell intensity and 300 hPa geopotential height

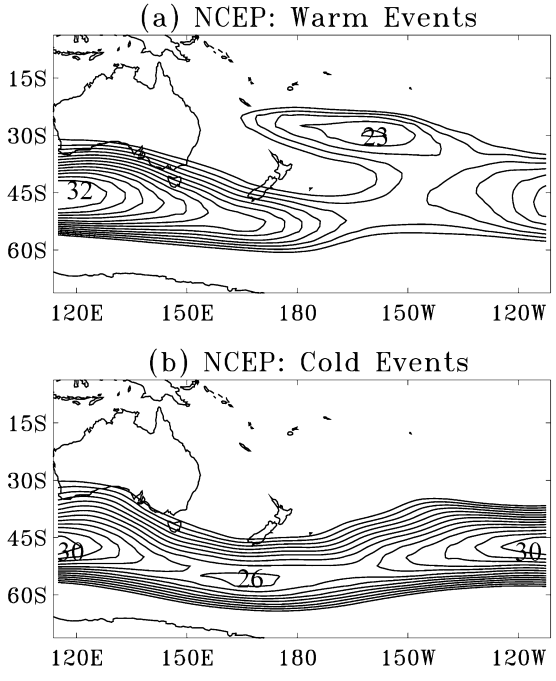

Fig. 4 **a** Warm and **b** cold DJF composites of zonal winds at 300 hPa, showing the westerly jet stream variations in the NCEP data. The contours are plotted at 1 ms^{-1} intervals starting from 18 ms^{-1}

warm-composite vortex-stretching term at 300 hPa (Fig. 5a) shows a strong cyclonic vorticity source in the latitude belt of 30–45°S. This is clearly associated with the descending branches of the Hadley and Ferrel circulations in this region. The advection of absolute vorticity by the divergent wind (Fig. 5b) has its maximum value in the subtropics. This coincides with the Hadley 300 hPa outflow from the convectively active regions during December–February. It is clear from the Fig. 5a–c that the vortex-stretching term contribution to the total effective Rossby wave source dominates between 30–45°S, suggesting the domination of upper level convergence in this region. The warm minus cold composite of the Rossby wave source (Fig. 5d) also indicates the relatively increased subsidence during El Niño years in this region.

3.3 Transient response

3.3.1 Storm track variations

The effect of the quasi-stationary Rossby wave anomalies is to alter the strength and location of the westerly jet in the southern Pacific in response to the warm phase of the ENSO cycle (Fig. 4a). One might, then, expect these changes in the jet stream to influence the existence of the extratropical cyclones in this region. This has been investigated using 300 hPa transient eddy kinetic energy. A region of maximum transient eddy kinetic energy is associated with an increased synoptic scale wave

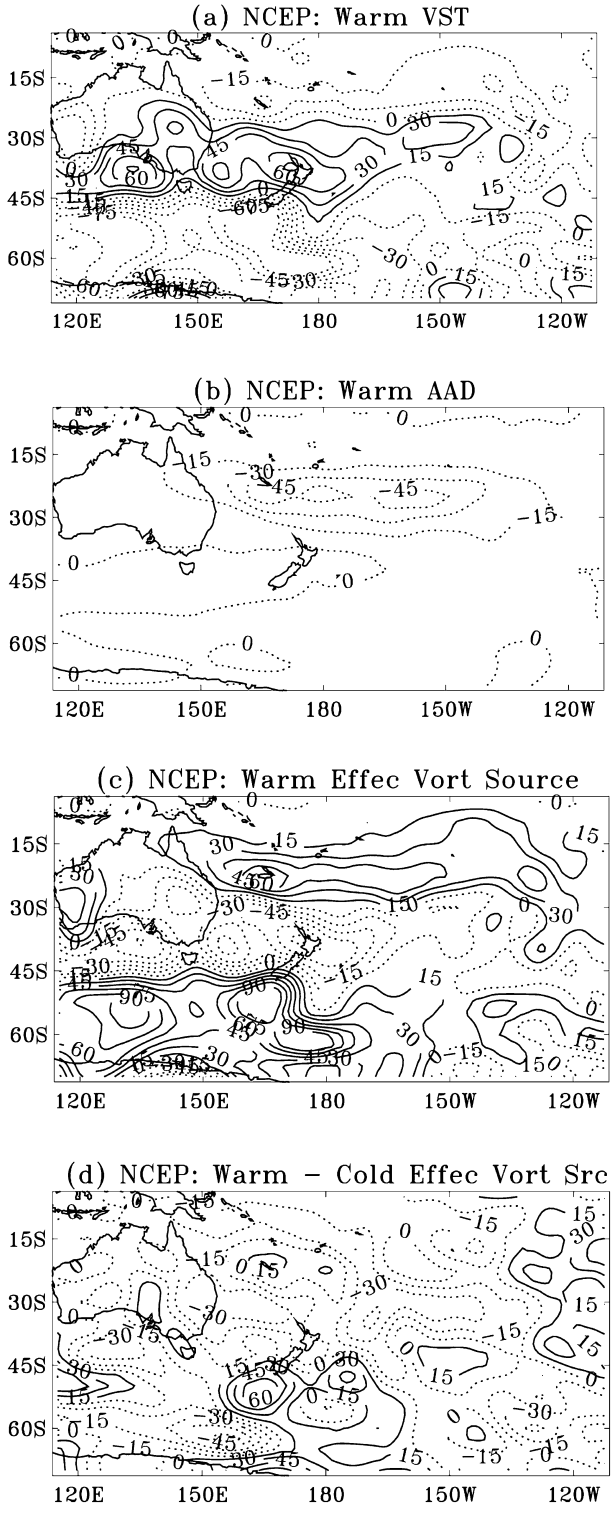

Fig. 5 **a** Warm composite of vortex stretching term $\overline{(\xi+f)\nabla\cdot V_\chi}$ at 300 hPa. **b** Warm composite of advection of absolute vorticity by divergent wind $\overline{V_\chi\cdot\nabla(\xi+f)}$. **c** Total effective Rossby wave source $\bar{S}$ composite for warm case. **d** Same as **c** but for warm minus cold case. All are in units of 10^{-12} s^{-2}. Negative contours are *dotted*

activity, which is referred to as the "storm track". The climatological shape of the storm track during DJF is markedly zonal in character (not shown), unlike in the

north Pacific and north Atlantic oceans where the tracks are deflected polewards at their exit regions (Orlanski 1998). The observed location of the storm track in our analysis is at about 50°S, which agrees fairly well with that obtained by Trenberth (1991) for January, using the European Centre for Medium Range Weather Forecasts (ECMWF) reanalyses data, for the period 1979–1989.

During La Niña years the extratropical storm track activity is largely guided by the westerly jet stream (compare midlatitude areas of negative correlation, shaded in Fig. 6, with the jet stream location of Fig. 4). During El Niño years the northern branch of the divided jet stream northeast of NZ plays a more active role in influencing storms in this region. The significantly increased storm activity during El Niño (La Niña) years in the subtropical marine latitudes east (west) of the dateline coincides with the location of the South Pacific Convergence Zone (SPCZ), where there is large-scale convergence and high sea surface temperatures.

3.3.2 High frequency forcing of the mean flow

Here we investigate the large-scale circulation that could arise from the high frequency forcing in the storm track region. For this purpose, the streamfunction tendencies due to anomalous transient vorticity flux convergences have been calculated for synoptic scale motions (see Subsect. 2.5). The HF transients we found in the southern Ocean are comparable to those found by Held et al. (1989) using a GCM data at 200 hPa. The subseasonal transients on all time scales from two days to a season may also play a role on influencing the mean flow. However here we confine our discussion only to the HF transients, since their role is more clearly defined in our analyses.

The positive (negative) streamfunction tendencies locally induce a cyclonic (an anticyclonic) circulation in the Southern Hemisphere. During El Niño years, the negative tendencies are found on the northern side of the westerly jet stream, with positive tendencies on the southern side (Fig. 7a). Thus the influence of HF transients on the jet stream is to intensify the westerlies, particularly in the areas west of the dateline where the North–South streamfunction tendency gradients are stronger. In the region east of the dateline the streamfunction tendency gradients are considerably weaker, consistent with the diffluence area (150°W and 50°S) of the jet stream (see Fig. 4a). During La Niña years, the interface between the negative and positive streamfunction tendencies are found further polewards (Fig. 7b), consistent with the more southerly location of the westerly jet stream (see Fig. 4b). Also the stronger streamfunction tendency gradients west of the dateline are oriented in the southwest–northeast direction (Fig. 7b), deflecting the westerlies polewards southwest of NZ (Fig. 4b). This is consistent with a result of Orlanski (1998) that the Northern Hemisphere climatological mean flow is deflected polewards by the HF transients.

To clarify the picture and further confirm the role of HF transient eddies in forcing the quasi-stationary mean circulation, Fig. 7 was redrawn after removing the background climatology and zonal means, and superimposed over the corresponding 300 hPa height anomalies (Fig. 8). During both the El Niño and La Niña events the streamfunction tendencies are almost in phase with the height anomalies. The positive streamfunction

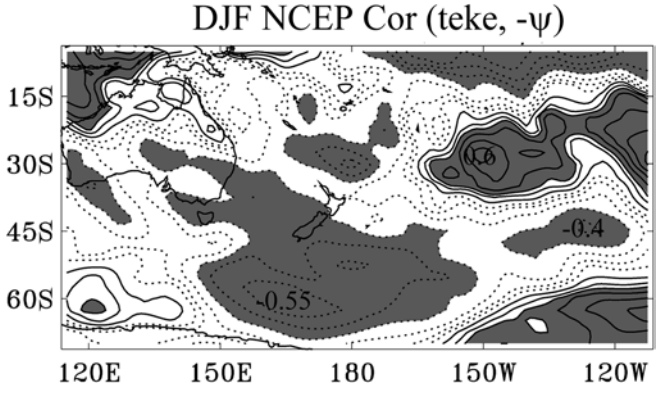

Fig. 6 Same as Fig. 2, but the correlations are between regional Hadley cell intensity and 300 hPa transient eddy kinetic energy

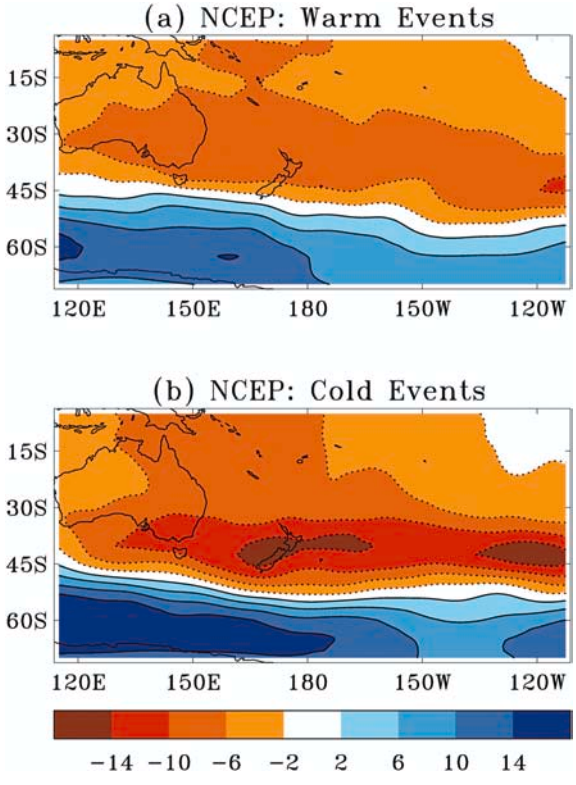

Fig. 7 Streamfunction tendencies in the NCEP data at 300 hPa due to high frequency transient vorticity flux convergences for **a** warm events and **b** cold events. Contours are in units of $m^2\ s^{-2}$. Contour levels are shown at the *bottom of the figures*. The negative contours are *dotted*, and the zero contours are not shown

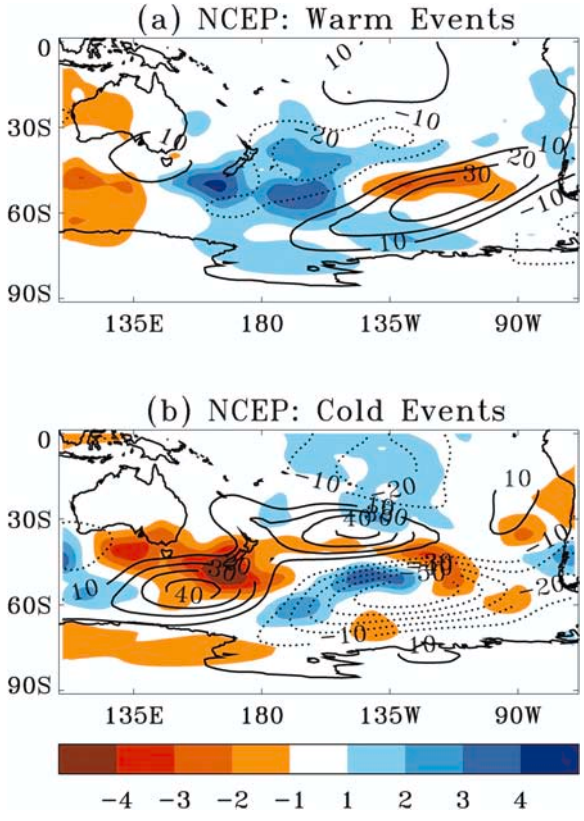

Fig. 8 Geopotential height anomalies (contours) and anomalous streamfunction tendencies due to high frequency transient vorticity forcing (*solid contours*) for **a** warm events and **b** cold events from the NCEP reanalyses at 300 hPa. The corresponding zonal means are removed. The height anomalies are contoured at ±10, ±20, ±30, ±40, and ±50 m. Contour levels for high frequency transient forcing are shown at the *bottom of the figures*. Note the strong correlation between height anomalies and transient eddy forcing in the southern extratropics

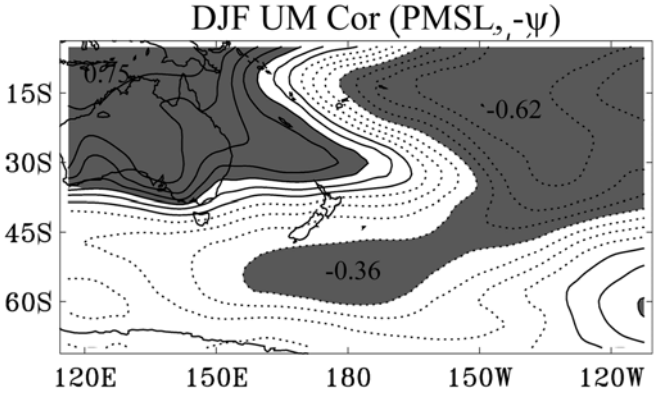

Fig. 9 Same as Fig. 2, but for the model

tendency (blue shading in Fig. 8), which induces a cyclonic circulation, overlaps with the negative 300 hPa height anomalies. As one would expect the height anomalies are found slightly to the east (downwind) of the transient forcing.

In summary, the mid-latitude HF eddies in the southern Pacific appear to influence the quasi-stationary mean circulation in this region, as concluded by Hoerling and Ting (1994) and Orlanski (1998) for the PNA region.

4 Unified Model simulations of the El Niño-related variability

4.1 Interannual variations

We now repeat many of the previous analyses and figures, but this time using the UM atmospheric simulations driven by observed sea surface temperatures over 1960–1994. The simulated contemporaneous correlations between ψ and PMSL have a north–south gradient over NZ (Fig. 9), slightly different from the northwest–southeast gradient found in the NCEP reanalyses of observations (Fig. 2). Thus, the UM accelerates (decelerates) westerlies in response to the increased (decreased) intensity of the regional Hadley cell associated with the El Niño (La Niña) events. The differing characteristics of the correlation structures found in the model may be attributed to the model's inability to simulate the correct shape and geographical location of the extratropical quasi-stationary Rossby wave anomalies (Fig. 10). The model responds reasonably well to the enhanced tropical Pacific convection by simulating appropriate upper level divergence in the equatorial region. However, the alternating high and low streamfunction anomalies in the southern Pacific resulting from the Rossby wave response are too zonal in character, and are displaced too far eastward (Fig. 10b). Later we show that these eastward placed anomalies are related to the existence of the HF transient eddies in this region.

4.2 Warm and cold composites

4.2.1 Large-scale circulations

The warm and cold composites of the 300 hPa zonal winds show variations in the intensity and shape of the simulated jet stream (Fig. 11), very similar to those found in the observations (Fig. 4). The intensified branch of the jet stream northeast of NZ during El Niño years is consistent with the quasi-stationary anomalies simulated by the model (see Fig. 10b). However, there is no noticeable equatorward movement of the westerly jet stream in the model associated with the El Niño events. In general the model produces stronger westerlies compared to the NCEP observations, consistent with the results based on composites made using only the nino3.4 SST anomalies (Bhaskaran et al. 1999). The regional meridional circulations are found to be stronger than normal during El Niño years (not shown), similar to that seen in the observations (Fig. 5a–d). However the main strengthening of the regional Hadley cells during

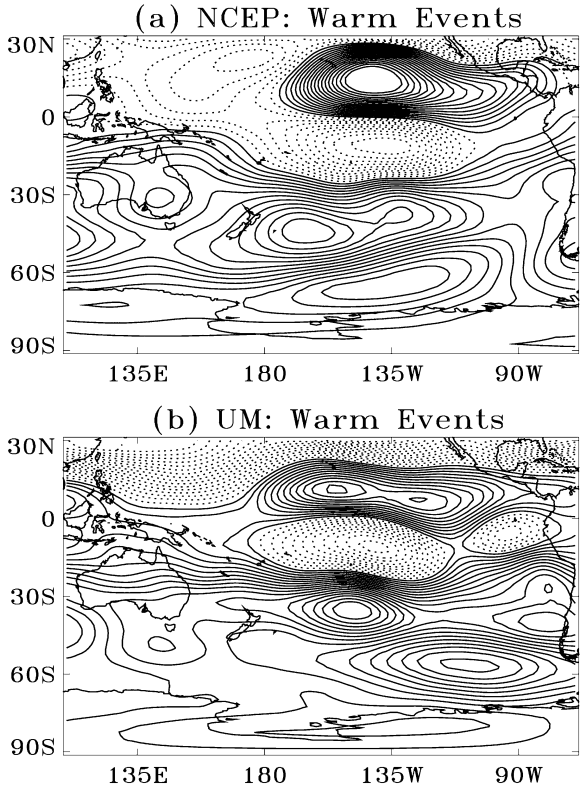

Fig. 10 Composited streamfunction anomalies for warm events at 300 hPa from **a** NCEP reanalyses and **b** unified model. Contour interval is 0.5×10^6 ms^{-1}. Negative contours are *dotted*

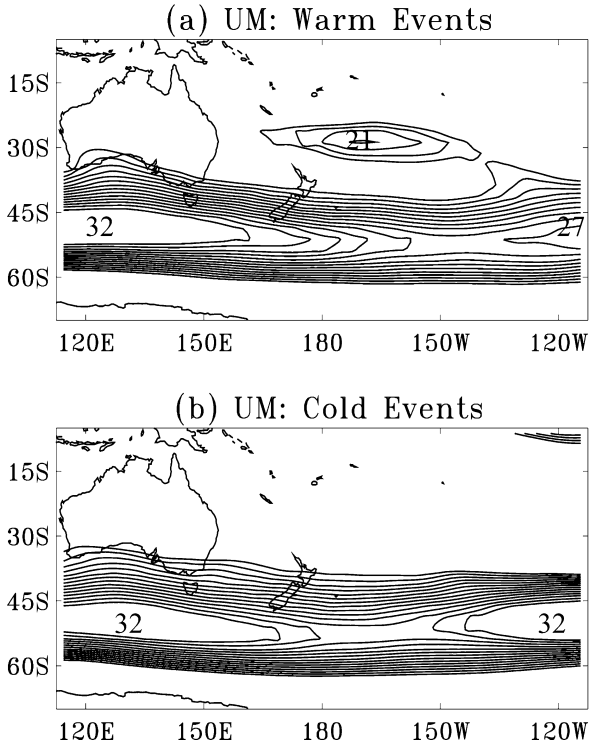

Fig. 11a, b Same as Fig. 4, but for the model. Contours are drawn at 1 ms^{-1} intervals starting from 18 ms^{-1}

El Niño years takes place further eastwards relative to the NCEP data, consistent with the eastward-displaced train of alternating high and low streamfunction anomalies in the model extratropics (Fig. 10b).

4.2.2 Precipitation

The unified model simulates the large-scale tropical circulation features associated with the El Niño events reasonably well. However, it fails to capture accurately the extratropical locations of the quasi-stationary anomalies resulting from the Rossby wave response (Fig. 10). Therefore the physical quantities, such as precipitation and surface air temperatures, simulated by the model are prone to relatively more errors in the extratropics. Nevertheless it is necessary to understand the model's ability to reproduce the observed precipitation patterns during El Niño and La Niña events in the ANZ region, if we want to use the unified model for a dynamical prediction of the seasonal means.

Here we consider the CRU and NCEP precipitation composites to compare against the model-simulated precipitation. The model simulates relatively lower precipitation over most of the Australian region during El Niño years (Fig. 12c). This is in fair agreement with the CRU and NCEP data sets, and in consistent with the results of Ropelewski and Halpert (1989). The model appears to capture the increased rainfall associated with the eastward migration of the SPCZ during El Niño years. The rainfall due to anomalous equatorial convection is also fairly well simulated by the model. The band of wetness seen in the model mid-latitudes during El Niño years is qualitatively similar to that found in the NCEP dataset, though the NCEP observations are far from reliable in this sector.

In summary, the model captures tropical and subtropical rainfall variations more convincingly than the extratropical rainfall features, consistent with the model's ability to simulate more accurate tropical circulation features in response to the equatorial Pacific convection.

4.3 Transient activity

4.3.1 Storm track variations in the model

The storm track changes in the subtropics simulated by the model in response to the regional Hadley cell intensity fluctuations associated with the El Niño and La Niña events (Fig. 13) are similar to that found in the observations (Fig. 6). However the model simulates an increase in the synoptic scale storm activity in the south Tasman Sea during El Niño years, whereas the NCEP data shows a significant decrease in the transient eddies. During La Niña years, the buildup of the storm activity in the north Tasman Sea at the climatological position of the SPCZ (Vincent and Silva Dias 1998) is more

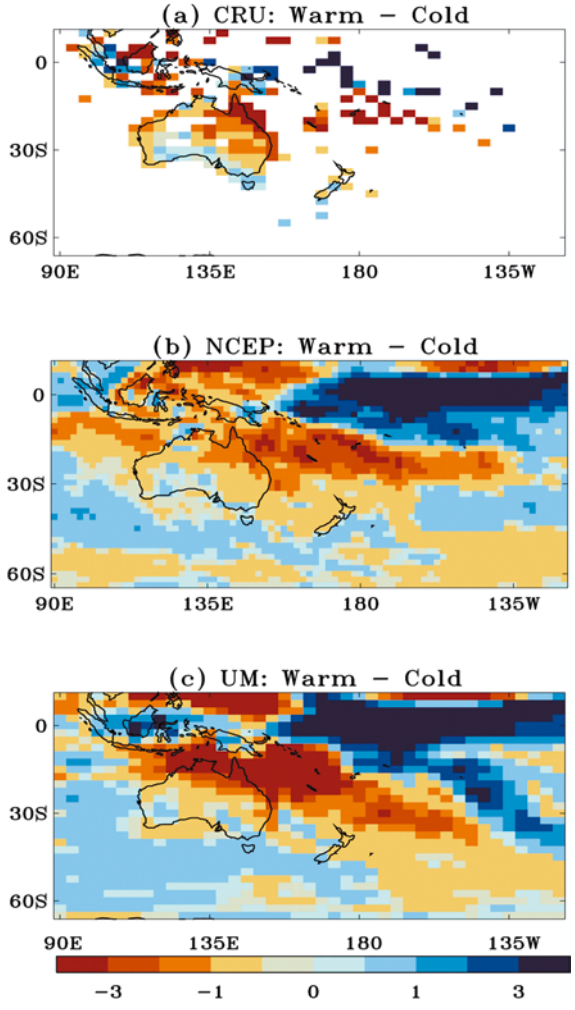

Fig. 12 Warm minus cold composite differences in precipitation (mm/day) for **a** CRU; **b** NCEP; and **c** unified model

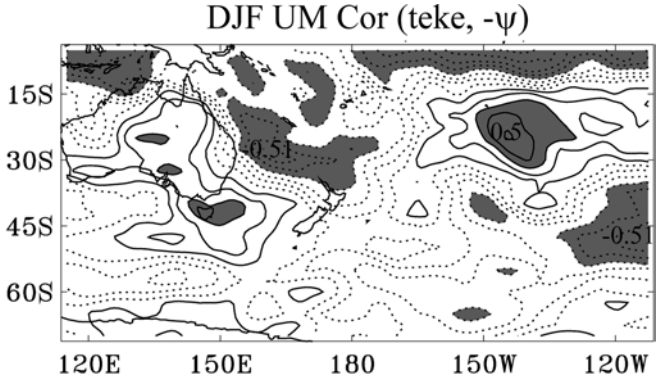

Fig. 13 Same as Fig. 2, but the correlations were calculated between regional Hadley cell intensity and 300 hPa transient eddy kinetic energy using unified model data

prominent in the model compared to the NCEP observations. However the existence of the transient eddies around the jet stream location is not as significant as it is found in the NCEP data. Thus, the model demonstrates its skill in reproducing the subtropical storm activity associated with the El Niño and La Niña events quite well, though it struggles to reproduce the extratropical synoptic scale wave activity associated with the jet stream during La Niña years.

4.3.2 Relationships between the storm track and mean flow

Although the extratropical storm activity is not accurately simulated by the model, there is a consistency between the existence of the HF transients and the extratropical westerlies in the extreme ENSO composites of the model, similar to that seen in the observations (see Subsect. 3.3.2). For example, the forcing exerted by the HF transients on the mean flow is to accelerate the westerly jet stream during both the El Niño and La Niña years (Fig. 14). The zonal character of the extratropical westerlies is consistently supported by the HF transients. The diffluence area in the jet experiences the reduced eddy forcing, particularly during El Niño years. Figure 15 further supports the role of the HF transients in forcing the seasonal mean extratropical circulation hypothesized by Hoerling and Ting (1994) for the PNA region. The striking similarity between the observations (Figs. 7 and 8) and model (Figs. 14 and 15) in relating the HF transients and the extratropical circulation anomalies increases our confidence in the role of the HF transients in maintaining the extratropical seasonal mean circulation in the southern Pacific, though it is not possible to study the cause and effect from the current analysis (see later).

5 Summary and conclusions

A detailed analysis of the impact of the El Niño – Southern Oscillation (ENSO) on the seasonal mean circulation and on the intraseasonal variability on synoptic time scales in the southern Pacific region has been carried out using the National Center for Environmental Prediction (NCEP) reanalyses data. We have also investigated the interaction of the synoptic scale transient eddies with the seasonal mean circulation with a view to understanding the level of influence the transient eddies exert on the mean flow during the selected El Niño and La Niña events. Subsequently the ability of a fully comprehensive general circulation model (GCM) developed at the United Kingdom Meteorological Office (UKMO), known as the unified model (UM), to reproduce the observed anomalous circulation features on both the seasonal and synoptic time scales associated with the ENSO phenomenon has also been assessed.

The western tropical Pacific regional Hadley cell intensity has been used as an El Niño index to classify the warming and cooling years for our composite analysis. The classical relationship between the regional Hadley cell and the warm-phase ENSO cycle circulation anomalies described by Bjerknes (1966, 1969), that the

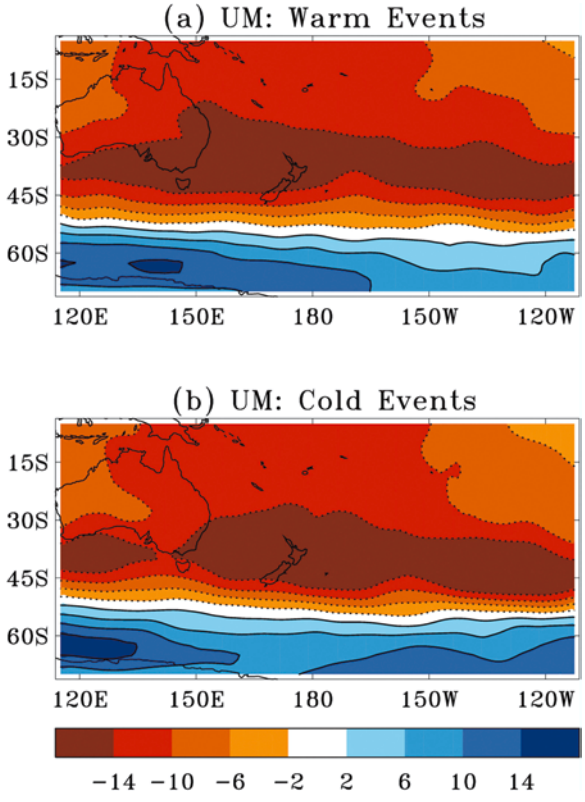

Fig. 14a, b Same as Fig. 7, but for the model

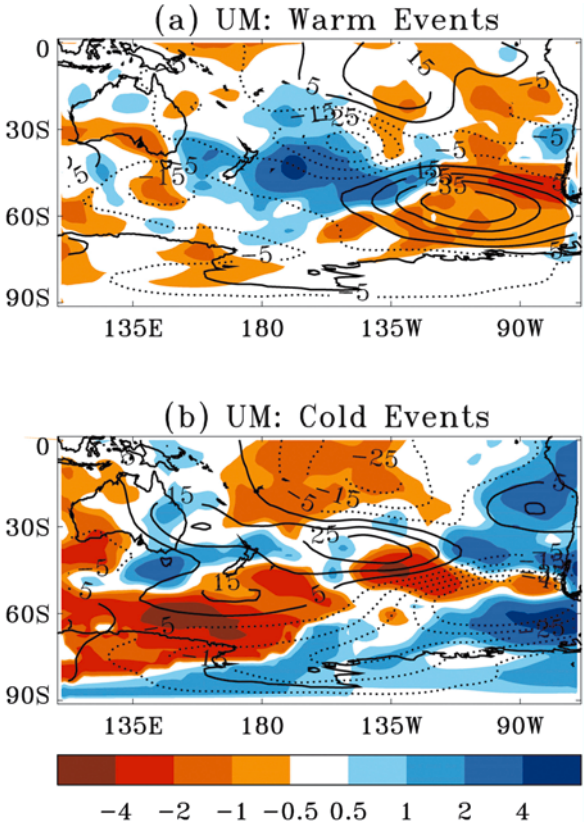

Fig. 15a, b Same as Fig. 8, but for the model

positive equatorial Pacific sea surface temperature (SST) anomalies drive stronger than normal regional Hadley cell in the affected longitudes, holds good during most of the El Niño years. However there were cases during which the relationship failed. This may be because the regional Hadley cells were perhaps influenced by the peculiar geometrical shape and magnitude of the SST anomalies during those years.

During El Niño years the regional Hadley cell in the tropical Pacific acts as a vehicle fuelled by the positive SST anomalies to produce a tropical upper level divergence and subtropical upper level convergence to excite a train of Rossby waves. This feature is consistently simulated by the UM except that the quasi-stationary anomalies in the extratropics resulting from the Rossby wave response are found about 30° longitude eastwards relative to the observations (Fig. 10). This may be because the Rossby wave response in the model has been influenced by the stronger extratropical westerlies found at upper levels in the model (Bhaskaran et al. 1999).

The observational analysis reveals that the extratropical westerly jet stream moves equatorwards during El Niño years. The split in the jet over the northeast of New Zealand (NZ) is also prominent. The variations in the storm track associated with the El Niño and La Niña events are largely related to the east–west migration of the South Pacific Convergence Zone (SPCZ) in the subtropics. The storms are largely guided by the northern branch of the jet stream in the areas northeast of NZ during El Niño years, and by the southern branch of the jet stream during La Niña years (Fig. 6). The model captures these observed storm track variations reasonably well, especially the eastward migration of the HF transients during El Niño years (Fig. 13). However it struggles to reproduce the significant storm activity associated with the jet stream during La Niña years.

Our analyses of the NCEP (Figs. 7 and 8) and model data (Figs. 14 and 15) indicate a strong relationship between the HF forcing and the quasi-stationary circulation anomalies during both the El Niño and La Niña years, though the quasi-stationary circulations in the model are slightly different from the observations. However, it is difficult to prove whether the HF transients maintain the time-mean circulation, or whether the HF transients exist because of the favourable conditions created by the seasonal mean circulation. Nevertheless the current observational analysis, supported by the model results and the results of Hoerling and Ting (1994) for the PNA region, increases our confidence in the role of the HF transients in forcing the quasi-stationary circulation in the southern Pacific. However we understand that a set of numerical experiments similar to those of Hoerling and Ting (1994) under idealized conditions are necessary for a concrete conclusion, which may be addressed in a future study.

Acknowledgements This research was funded by the New Zealand Foundation for Research, Science and Technology under contract C01X0030. The UK Meteorological Office supplied the unified model to NIWA. The authors would like to thank the National

Center for Environmental Prediction (NCEP) for providing their recent reanalyses data, and Dr. M. Hulme at the Climate Research Unit, East Anglia, UK for supplying the gridded observed precipitation data. We are grateful to M. Revell and an anonymous reviewer for their helpful comments.

References

Bhaskaran B, Jones RG, Murphy JM, Noguer M (1996) Simulations of the Indian summer monsoon using a nested regional climate model: domain size experiments. Clim Dyn 12: 573–587

Bhaskaran B, Mullan AB, George SE (1999) Modelling of atmospheric climate variations at NIWA. Weather Clim 19: 23–36

Bjerknes J (1966) A possible response of the atmospheric Hadley circulation to equatorial anomalies of ocean temperature. Tellus 18: 820–829

Bjerknes J (1969) Atmospheric teleconnections from the equatorial Pacific. Mon Weather Rev 97: 163–172

Cullen M (1993) The unified forecast/climate model. Meteorol Mag 122: 81–94

Gordon ND (1986) The Southern Oscillation and New Zealand weather. Mon Weather Rev 114: 371–387

Held IM, Lyons SW, Nigam S (1989) Transients and the extratropical response to El Niño. J Atmos Sci 46: 163–174

Hoerling MP, Ting M (1994) Organization of extratropical transients during El Niño. J Clim 7(5): 745–766

Hoerling MP, Kumar A, Zhong M (1997) El Niño, La Niña, and the nonlinearity of their teleconnections. J Clim 10: 1769–1786

Hulme M (1992) A 1951–80 global land precipitation climatology for the evaluation of general circulation models. Clim Dyn 7: 57–72

Kane RP (1998) Extremes of the ENSO phenomenon and Indian summer monsoon rainfall. Int J Climatol 18: 775–791

Latif M, Anderson D, Barnett T, Cane M, Kleeman R, Leetmaa A, O'Brien J, Rosati A, Schneider E (1998) A review of the predictability and prediction of ENSO. J Geophys Res 103: 14,375–14,393

McBride JL, Nicholls N (1983) Seasonal relationships between Australian rainfall and the Southern Oscillation. Mon Weather Rev 111: 1998–2004

Mullan AB (1996) Non-linear effects of the southern oscillation in the New Zealand region. Austral Meteorol Mag 45: 83–99

Murakami M (1979) Large-scale aspects of deep convective activity over the GATE area. Mon Weather Rev 107: 994–1013

Orlanski I (1998) Poleward deflection of storm tracks. J Atmos Sci 55: 2577–2602

Parker DE, Folland CK, Jackson M (1995) Marine surface temperature: observed variations and data requirements. Clim Change 31: 559–600

Philander SG (1990) El Niño, La Niña and the Southern Oscillation. Academic Press, San Diego pp 289

Power S, Tseitkin F, Torok S, Lavery B, Dahni R, McAvaney B (1998) Australian Temperature, Australian rainfall and the Southern Oscillation, 1910–1992: coherent variability and recent changes. Austral Meteorol Mag 47(2): 85–101

Rasmusson EM, Mo K (1993) Linkages between 200-mb tropical and extratropical circulation anomalies during the 1986–1989 ENSO cycle. J Clim 6: 595–616

Renwick JA (1998) ENSO-related variability in the frequency of south Pacific blocking. Mon Weather Rev 126: 3117–3123

Renwick JA, Revell MJ (1999) Blocking over the south Pacific and Rossby wave propagation. Mon Weather Rev 127: 2233–2247

Ropelewski CF, Halpert MS (1989) Precipitation patterns associated with the high index phase of the Southern Oscillation. J Clim 2: 268–284

Sardeshmukh PD, Hoskins BJ (1988) The generation of global rotational flow by steady idealized tropical divergence. J Atmos Sci 45: 1228–1251

Stratton RA (1999) A high resolution AMIP integration using the Hadley Centre model HadAM2b. Clim Dyn 15: 9–28

Trenberth KE (1991) Storm tracks in the Southern Hemisphere. J Atmos Sci 48: 2159–2178

Trenberth KE, Branstator GW, Karoly D, Kumar A, Lau NC, Ropelewski C (1998) Progress during TOGA in understanding and modeling global teleconnections associated with tropical sea surface temperatures. J Geophys Res 103: 14,291–14,324

Vincent DG, Silva Dias PS (1998) Pacific Ocean. In: Karoly DJ, Vincent DG (eds) Meteorology of the Southern Hemisphere. American Meteorological Society, Boston, pp 101–117

Walker GT, Bliss EW (1937) World weather. VI Mem R Meteorol Soc 4: 119–139